Numerical performance assessment of a new wave energy conversion system

André F.L. Governo, José M.C.S. André, João C.C. Henriques, Luís M.C. Gato

Abstract—**The greater wave energy content in deeper waters has motivated substantial research in offshore wave energy converters (WECs). However, the existing WECs are hindered by large initial costs, primarily attributed to the demanding mechanical workloads they endure. In response, this paper presents an innovative wave energy conversion system, developed at IST, tailored for deep waters (approximately 20 to 50 meters). The system employs a floater and ballast, suspended by cables, and stands apart with its use of membranes instead of a rigid structure, significantly reducing the initial investment costs compared to conventional solutions. To evaluate the system's performance, a simplified numerical model in the time-domain is developed, based on linear theory. We conduct a preliminary assessment of its capabilities under both regular and irregular wave conditions, the latter representing prevalent conditions along the western coast of Portugal. Furthermore, we investigate the influence of the ballast mass on the system's efficiency. The results highlight the non-linear behavior during the floater's ascending phase and emphasize the significant impact of the ballast's mass on power production. By offering a simpler alternative for deep-water applications and shedding light on the system's behavior under varying wave conditions, this solution contributes to the advancement of cost-effective wave energy conversion technologies.**

Index Terms—**Wave Energy Converter, Deep water, Numerical model, Regular and Irregular waves, Time-domain**

I. Introduction

OFFSHORE wave energy converters (WECs) operating at few tens of meters of water depth benefit from greater energy resource availability and fewer deployment limitations and are inherently floating devices. Hence, they are of increased relevance in the wave energy sector.

Point absorber devices are a class of wave energy devices where energy production is often based on the relative motion between a floating body, whose characteristic size is considerably smaller than the wavelength, and a reference point. The reference point may be a submerged body, such as a ballast, or even the sea bottom, although the former is less attractive in deep waters because of the increased mechanical workloads. For the first, the moving elements can exhibit relative motion in different ways. For instance, in devices such as the PowerBuoy, the Wavebob and the IPS, the elements are mostly oscillating in heave [1], [2]. On the other hand, in converters like the SEAREV [3] and the Pelamis [4], there is relative rotation between the components.

The seabed poses several difficulties and limitations to the viability of the oscillating devices, as it is very expensive to build structures capable of withstanding high compression forces. Therefore, to make the device economically viable, it is important that all the structural elements that make up the floating system work mainly under tensile stresses. In this way, by significantly reducing the costs associated with the construction and maintenance of all the equipment, the cost-to-energy ratio is expected to become much more advantageous.

Based on these considerations, the solution of the WEC proposed in [5], developed at Instituto Superior Técnico (IST), consists of replacing the inertia of the seabed with that of a submerged body connected to the floater by cables, thus obtaining a reference that suffers much less from the action of the marine environment. The set of cables is wrapped around a drum inside the floater. The main advantage of the novel wave energy converter is that does not possess a rigid structure and is made essentially of membranes and cables. The floater is a pressurised water or gas coated with textile or thin sheet material that works only under tension. This component is therefore much lighter, cheaper and more flexible. Additionally, this configuration can also extract energy from the pitch and surge motions, whereas, in general, cables winded around drums interact only with the vertical movement of the floater.

The energy production cycle of the device can be divided in the following steps (see Fig. 1 for partial illustration). Every time the floater moves upwards under direct wave action, the ballast moves with it because a brake mechanism inside the floater blocks the drum. This process reduces the distance between the ballast and the floater, causing the cables between them to wrap around the drum. At a certain point, when the distance between the floater and the ballast reaches the design minimum, the brake is released and the cables unwind as the ballast descends. The drum inside the floater is then responsible for converting the relative motion between the ballast and the floater into rotary motion, driving a generator. Note that in this way the ballast lift can be "accumulated" over several wave cycles in a continuous process, as shown in Fig. 1. This description of the converter's operation is a

The first author was supported by FCT grant no. DFA/BD/07315/2021.

IDMEC, Instituto Superior Técnico, Universidade de Lisboa, Av. Rovisco Pais 1, 1049-001 Lisboa, Portugal

E-mail addresses:
andre.governo@tecnico.ulisboa.pt (André F.L. Governo),
jose.maria.andre@tecnico.ulisboa.pt (José M.C.S. André),
joaochenriques@tecnico.ulisboa.pt (João C.C. Henriques),
luis.gato@tecnico.ulisboa.pt (Luís M.C. Gato)

Digital Object Identifier:
https://doi.org/10.36688/ewtec-2023-260

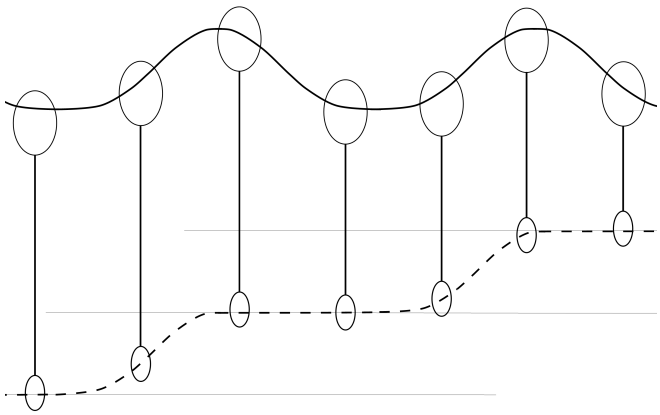

Fig. 1. Schematic of the WEC device during two wave periods.

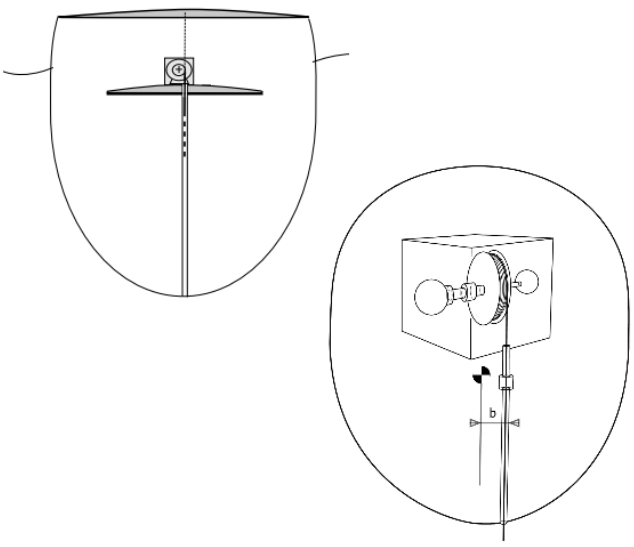

Fig. 2. Floater inside overview (left) and representation of cable's moment arm b, measured from the center of mass of the floater (right).

simplified summary, and for a fuller and more detailed explanation, please refer to the original reference [5].

In summary, the fact that it does not possess structural elements subjected to compression nor a hydraulic system, is a crucial aspect in significantly reducing the cost of the device in comparison with other floating WECs. Ocean waves are a free resource, and prioritising the reduction of the cost of energy production, rather than focusing solely on the energy produced in isolation, can increase economic viability.

This study aims to assess the performance of the presented wave energy conversion system by modeling its behaviour under different wave conditions and variable parameters to estimate energy production. The generated data plays a crucial role in validating the anticipated economic viability of the converter. To achieve this objective, a simplified numerical model is developed, focusing on the two main components of the system: a floater and a ballast mass, interconnected by rigid cables.

The paper is organized as follows. Section II describes the system and the mathematical framework (assumptions and modelling details). Next, the numerical results are presented in Section III, for regular and irregular conditions and with and without the ballast. Additionally, the mean power production of the wave energy converter is evaluated. Finally, the conclusions and future work appear in Section IV.

II. Numerical model

A. System description

The geometry of the floater consists of a cylindrical body buoy attached to a hemispherical calotte with the same radius, as shown in Fig. 2 on the left. In this model, the floater is connected to the submerged ballast by an approximately rigid cable. The ballast is therefore expected to act as a constraint on the overall motion of the floater. In addition, the cable is eccentric to the centre of mass of the floater, as shown in Fig. 2 on the right, and therefore induces moments on the floater. The hydrodynamic interaction between the ballast and the floater is neglected, as is the hydrodynamic interaction between the ballast and the waves. The approximation seems reasonable as the ballast is never close to the free surface.

We will assume a reference coordinate system fixed at the center of mass of the floater, having six degrees of freedom (DOFs). However, owing to the axisymmetry of the system, only three DOFs were considered: surge (mode 1), heave (mode 3) and pitch (mode 5). Moreover, linear wave theory and regular waves will be used. These details will be clearer in the following subsections.

B. Governing Equations

The general equations of motion in the time-domain for a WEC are represented by the balance of forces acting on the body, which, for this particular system, take the form,

$$(M_{ij} + A_{ij}^{\infty})\,\ddot{x}_j = F_{\mathrm{e},i} + F_{\mathrm{r},i} + F_{\mathrm{st},i} + F_{\mathrm{c},i}. \qquad (1)$$

Here x_j represents the device's motion in the degree-of-freedom j, M_{ij} is the inertia matrix associated with the floating body and A_{ij}^{∞} are the added mass terms at infinite frequency. Furthermore, on the right-hand side, the forces include the hydrodynamic excitation force F_{e}, the radiation force F_{c}, the hydrostatic restoring force F_{st} and the forces exerted by the cable F_{c}.

In this paper, the notation used is $\dot{x} = \mathrm{d}x/\mathrm{d}t$ for differentiation with respect to time. Additionally, the time dependence of the variables is omitted throughout.

Although the components i, j can vary between 1 and 6 for a general body, they only take the values of 1, 3 and 5 in this work since the other modes were neglected due to the axisymmetry of the problem (see above). Hence, the inertia matrix will have the following non-zero components: $M_{11} = M_{33} = m_{\mathrm{F}}$, and $M_{55} = I_{55}$, where m_{F} is the floater's mass and I_{55} is the moment of inertia w.r.t (with respect to) the y-axis. This value is given by

$$I_{55} = \frac{8}{15} m_{\mathrm{F}} R^2, \qquad (2)$$

where R is the radius of the floater.

The hydrostatic restoring force F_{st} is related with the deviation of the body's position away from equilibrium (thus, for no waves, $F_{\mathrm{st}} = 0$). The linearised version is computed from

$$\begin{aligned} F_{\mathrm{st},3} &= -\rho_{\mathrm{w}} g S_{\mathrm{F}} x_3, \\ F_{\mathrm{st},5} &= -\rho_{\mathrm{w}} g W_{55} x_5, \end{aligned} \tag{3}$$

where ρ_{w} is the water density, g is the acceleration of gravity, S_{F} is the area of the floater at the mean wave line (MWL) and W_{55} corresponds to the moment of inertia of the area, due to rotation,

$$W_{55} = \int_0^{2\pi}\int_0^R x_5^2 r \,\mathrm{d}r\mathrm{d}\alpha, \quad x_5 = r\sin(\alpha) \tag{4}$$

The interaction between the floating body and the wave can be decomposed into a diffraction problem, which quantifies the forces applied to the body by the incident and scattered waves, and a radiation problem, which accounts for the damping and inertia effects on the body induced by the generated waves. To address these phenomena, the mean wetted surface area is considered.

The radiation force F_{r} results from the body oscillating in still water (no incident wave) and is calculated from [6]

$$F_{r,i}(t) = -\int_{-\infty}^{t} K_{ij}(t-\tau)\,\dot{x}_j(\tau)\,\mathrm{d}\tau - A_{ij}^{\infty}\ddot{x}_j, \tag{5}$$

where K_{ij} is the impulse response function, that depends on the body's geometry and frequency. The kernel of the convolution integral is

$$K_{ij}(t) = \frac{2}{\pi}\int_0^{\infty} B_{ij}(\omega)\cos(\omega t)\,\mathrm{d}\omega. \tag{6}$$

Here B_{ij} represents the radiation damping coefficient and is associated with the energy dissipated by the waves generated by the floating body. Moreover, $A_{ij}^{\infty} = \lim_{\omega\to\infty} A_{ij}(\omega)$ is the added mass coefficient for the floater when the frequency goes to infinity. Prony's method [7] was employed in the calculation of the convolution integral, which evolves in a system of ODEs to be solved at each time step, that is

$$F_{\mathrm{r}} = \sum_{k=1}^{N} I_k, \tag{7}$$

with

$$\dot{I}_{\mathrm{r}} = \beta_{\mathrm{r}} I_{\mathrm{r}} + \alpha_{\mathrm{r}}\dot{x}. \tag{8}$$

A total of $N = 8$ exponentials were used. The function approximation and the corresponding error for the heave mode are depicted in Fig. 3. Consult [8] for more details.

The excitation force F_{e} is realized by solving the diffraction problem and represents the load acting on the fixed floating body subjected to the incoming wave. For a general case in linear water wave theory, it is calculated as a superposition of regular wave components, that is

$$F_{\mathrm{e},i} = \sum_{i=1}^{n} \Gamma(\omega_i)\, A_{\mathrm{w}_i} \cos(\omega_i t + \phi_i), \tag{9}$$

with

$$A_{\mathrm{w}_i} = \sqrt{2\Delta\omega_i, S_\zeta(\omega_i)} \tag{10}$$

$$\Delta\omega_i = (1 + \varpi\,\mathrm{rand}())\Delta\omega, \tag{11}$$

$$\omega_i = \omega_{i-1} + \frac{1}{2}(\Delta\omega_i + \Delta\omega_{i-1}), \tag{12}$$

and where $i = 2,\ldots,n$, Γ is the excitation force coefficient (frequency dependent) per unit wave amplitude, A_{w} is the wave amplitude, ω is the angular frequency, and ϕ is the wave phase. For the setup, $n = 300$ frequency components, $\omega_1 = 0.1$ and $\mathrm{rand}()$ is a random number generator between 0 and 1. Non-equally spaced frequencies are used to prevent the irregular spectrum to repeat itself at multiples, as demonstrated in previous works [9]. For the wave energy density spectrum, the Pierson-Moskowitz spectrum was used [10]

$$S_\zeta(\omega) = 262.9 H_{\mathrm{s}}^2 \omega^{-5} T_{\mathrm{e}}^{-4} \exp\left(-1054\omega^{-4}T_{\mathrm{e}}^{-4}\right), \tag{13}$$

where T_{e} is the energy period and H_{s} is the significant wave height.

To compute the energy annual output of the WEC device, a set of 14 different sea states (120 min each) was considered, related to the wave conditions for a location off the western coast of Portugal, in the Atlantic ocean. Each state state is defined by different values of H_s and T_e, together with the frequency of occurrence ϕ [9].

Finally, the force exerted by the cable F_{c} is given by

$$F_{\mathrm{c}} = m_{\mathrm{b}}(\ddot{x}_{\mathrm{b}} + g'), \tag{14}$$

where $g' = (1 - \rho_{\mathrm{w}}/\rho_{\mathrm{b}})\,g$ is the equivalent acceleration of gravity taking into account the buoyancy effect. In the formulas above, m_{b} represents the ballast's mass, ρ_{b} is the ballast's density and $\ddot{x}_{\mathrm{b}}$ is the acceleration of the ballast. Moreover, a rigid cable is assumed, hence $\ddot{x}_{\mathrm{b}} = \ddot{x}_i$ $(i = 3, 5)$.

The frequency-dependent hydrodynamic coefficients A_{ij}^{∞}, B_{ij}, Γ_i, and the phase response ϕ_i were determined using WAMIT [11]. A complete description of the methods used to compute the hydrodynamic coefficients as well as specific mesh information are referred to [12].

The governing equations that dictate the buoy's motion in time for surge (x_1), heave (x_3) and pitch (x_5) are then

$$(m_{\mathrm{F}} + A_{11}^{\infty})\,\ddot{x}_1 + J x_1 + A_{15}^{\infty}\ddot{x}_5 = F_{\mathrm{d},1} - F_{r,1}, \tag{15}$$

$$(m_{\mathrm{F}} + A_{33}^{\infty} + m_{\mathrm{b}})\,\ddot{x}_3 + \rho_{\mathrm{w}} g S x_3 = F_{\mathrm{d},3} - F_{r,3} - F_{\mathrm{c},3}, \tag{16}$$

$$\left(I_{\mathrm{yy}} + A_{55}^{\infty} + m_{\mathrm{b}} b^2\right)\ddot{x}_5 + \rho g W_{55} x_5 + A_{51}^{\infty}\ddot{x}_1 = F_{\mathrm{d},5} - F_{r,5} + F_{\mathrm{c},5}. \tag{17}$$

Note that, according with the operational mode of the system, the ballast's mass will only by accounted in an ascending phase ($\dot{x}_3 > 0$), otherwise it will be zero (released).

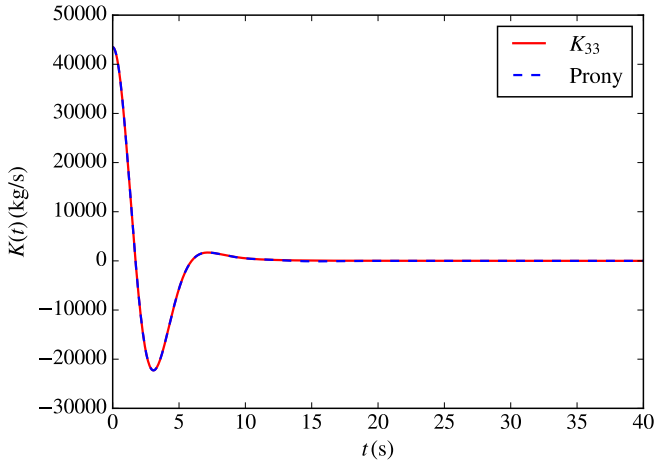

(a) Impulse response function fitting.

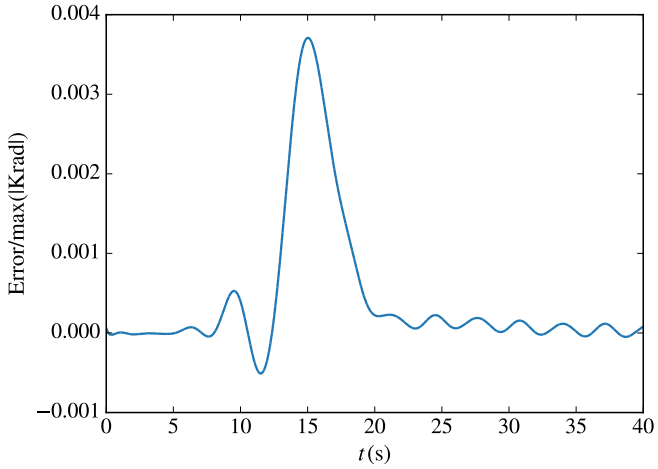

(b) Relative error against maximum value.

Fig. 3. Impulse response function fitting and relative error for heave ($K_{33}(t)$) with $N = 8$ and $t \in [0 - 40]$.

A smooth start of the simulation was imposed by using a asymptotic cubic function $R(t)$ for the equivalent of 10 wave periods T. The ramp function has the form

$$\begin{aligned} R(t) &= 3r^3\left(6r^2 - 15r + 10\right), \\ r &= \frac{t}{t_{\text{end}}}, \\ R(0) &= 0, \\ R(t_{\text{end}}) &= 1, \end{aligned} \tag{18}$$

where $t_{\text{end}} = 10T$.

The equations of motion are evolved in time using a third-order Runge-Kutta integrator.

III. Results and Discussion

The geometry of the floater has $R = 6\,\text{m}$ hemisphere and draft $D = 14.4\,\text{m}$. The mass density of the water ρ_{w} and the ballast ρ_{b} are $1025\,\text{kg/m}^3$ and $2500\,\text{kg/m}^3$, respectively. The distance between the center of mass of the floater and the cable b (in a static equilibrium position) is 1 m. The time step for the simulations was $\Delta t = 0.01\,\text{s}$ (constant). A complete list of the numerical model parameters is detailed in Table I.

The results are shown for a time window where the floater's response has stabilized, avoiding the initial transients. Only the results for heave (mode 3) are shown since they are the only ones needed for energy production calculations.

TABLE I
Relevant physical and numerical variables.

Symbol	Quantity	Value
R	Hemisphere radius	6 m
D	Floater's draft	14.4 m
ρ_{w}	Density of water	$1025\,\text{kg/m}^3$
ρ_{b}	Density of ballast	$2500\,\text{kg/m}^3$
A_{w}	Wave amplitude	1 m
T_{w}	Wave period	[5-14] s
m_{b}	Mass of the ballast	{50000, 70000} kg
b	Moment arm	1 m
Δz	Max. distance FB	40 m
Δt	Time step	0.01 s

FB denotes floater to ballast.

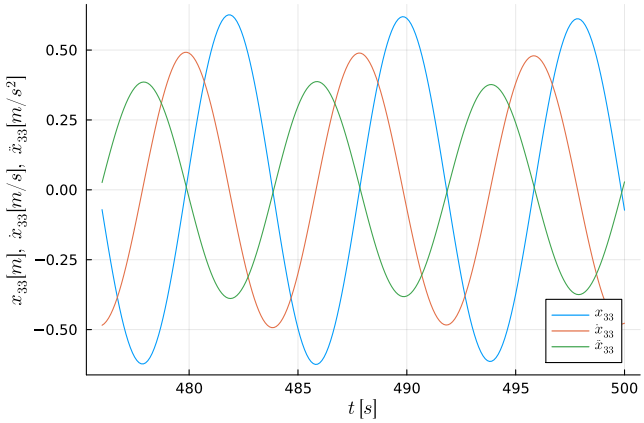

Fig. 4. Position, velocity and acceleration of the floater in heave, with no ballast ($m_{\text{b}} = 0$ kg).

A. Regular waves: floater without the ballast

The results concerning the behaviour of the floater without the ballast are shown in Fig. 4, for position (x_{33}), velocity ($\dot{x}_{33}$) and acceleration ($\ddot{x}_{33}$). Without the ballast, the floater's mean position is at the MWL from static equilibrium, reaching a maximum amplitude of 0.57m.

B. Regular waves: floater with the ballast

Let us now include the ballast into the system and evaluate its effect. As previously discussed, the ballast will only act when the floater is ascending with the waves, therefore, its effect and variation will be non-linear. The ballast will now act as a constraint to the floater´s motion increasing the inertia of the system, particularly in mode 3, since the cable is vertical. In reality, it should be almost vertical but not completely, since there will be surge and pitch movements. However, that effect is neglected in the current numerical model. Furthermore, the cable is not aligned with the center of mass connecting the ballast to the floater and, thus it will produce a positive rotation.

Two different ballast masses are studied: $m_{\text{b}} = 50000\,\text{kg}$ and $m_{\text{b}} = 70000\,\text{kg}$. The regular waves are

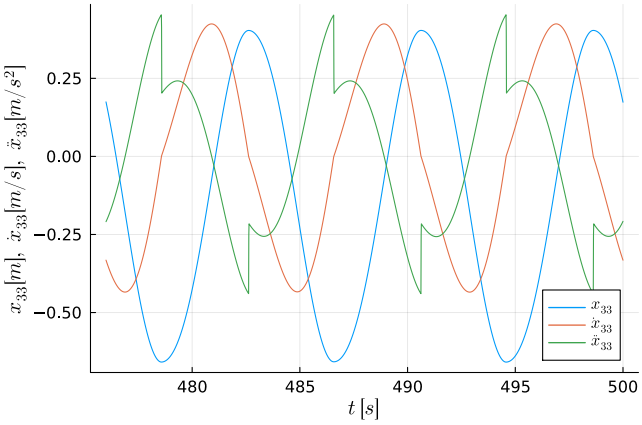

(a) $m_\mathrm{b} = 50000$ kg

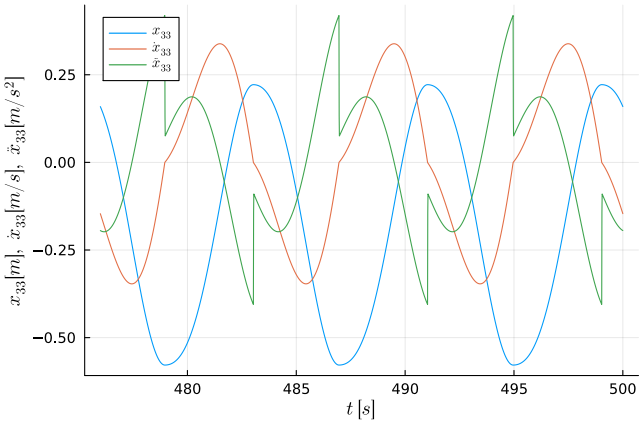

(b) $m_\mathrm{b} = 70000$ kg

Fig. 5. Position (x_{33}), velocity ($\dot{x}_{33}$) and acceleration ($\ddot{x}_{33}$) of the floater in heave, for different ballast masses m_b.

characterized by a sea state of $T_\mathrm{w} = 8\,\mathrm{s}$ and $A_\mathrm{w} = 1\,\mathrm{m}$. The results are presented in Fig. 5.

As shown in Fig. 5 (a), in the time instant where the floaters begins its ascending phase (velocity $\dot{x}_{11} > 0$), at the lowest position of the floater, the ballast is actuated and the slope of the velocity curve decreases due to the increase of inertia in the system. Hence, the peak position of the floater in heave decreases to $0.28\mathrm{m}$. Additionally, there is a non-continuous decrease of acceleration due to the additional inertia terms, hence the force is discontinuous. When the floater reaches its peak point (maximum), the ballast is released and the floater acts as a sole system again.

For an increased ballast mass (Fig. 5 (b)), this effect is more pronounced as expected and the floater's peak position is shorter. As mentioned before, it has direct implications in the energy production since the floater (and, consequently, the ballast) travel less distance in each wave period. However, the energy content of the ballast is larger since it is heavier.

C. Regular waves: Power production of the device

The results from last subsections can be used to calculate the energy and power production of the wave energy converter, by measuring the potential energy stored in the ballast, as it rises with the floater. That energy is

$$E_\mathrm{b} = m_\mathrm{b} g' \Delta z, \tag{19}$$

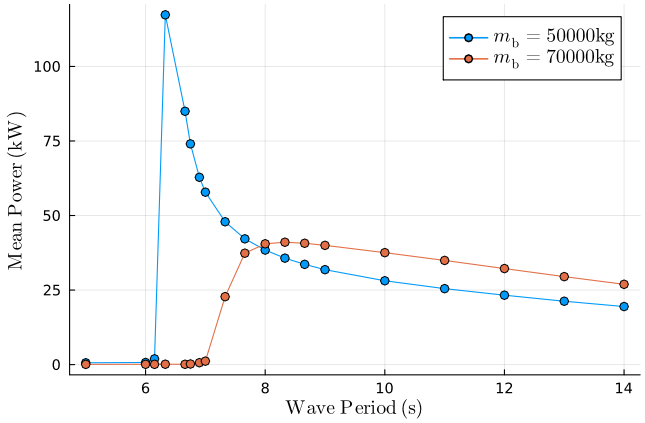

Fig. 6. Mean power during a full energy production cycle, for different ballast masses m_b and varying wave periods T_w.

where Δz corresponds to the distance travelled by ballast from the lowest point to the peak point. Then, the potential energy stored in the ballast increases with Δz. Additionally, if Δz is constant, the energy can be increased via the mass of the ballast (m_b). This increase in potential energy is not necessarily related with an increase of the mean power production, since a heavier ballast will take longer to reach the same distance, as demonstrated by the results of the previous subsection.

Hence, the power produced is calculated through

$$P_\mathrm{b} = \frac{E_\mathrm{b}}{\Delta t}, \tag{20}$$

where Δt is time required the lift the ballast from the lowest position to the peak point.

By using the position curves (x_{33}) in heave, we can calculate the difference between the maximum and minimum of the curves. It is also know that this difference is achieved in half of the period. Therefore, the calculations are straightforward. A distance of $\Delta z = 40\,\mathrm{m}$ is assumed between the ballast's minimum and maximum operational positions. Under these assumptions, the mean power produced by the device in regular waves is presented in Fig. 6.

The results clearly emphasize the system's non-linearity when the ballast is included in the model. For wave periods $T_\mathrm{w} < 8\,\mathrm{s}$, the lower ballast mass presents higher power output, with a peak power of $P_\mathrm{b} = 120\,\mathrm{kW}$. However, for larger periods, the greater ballast mass slightly outperforms for the entire range. Moreover, the resonance peak is lost due to the very large inertia of the system and the range at which the device could operate is moved towards higher periods.

D. Irregular waves

The results pertaining to irregular wave conditions are presented here. Wave conditions for a location off the western coast of Portugal are contemplated through a Pierson-Moskowitz spectrum with a sea-state of $H_\mathrm{s} = 2.8\,\mathrm{m}$ and $T_\mathrm{e} = 8.14\,\mathrm{s}$. This single case has the same average energy as the tabulated conditions from [8]. In calculating the mean energy production of the system, a 20 min series in the same time window was considered.

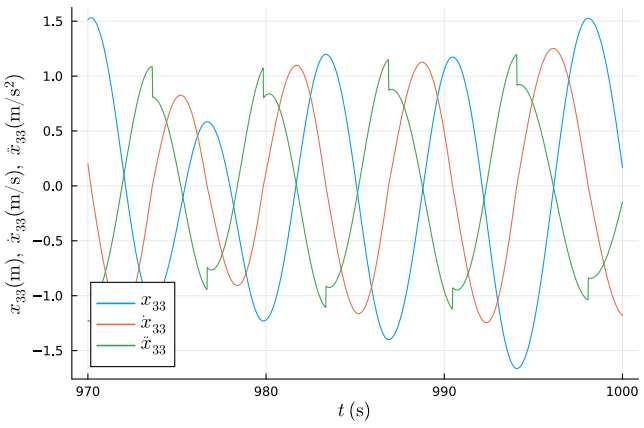

Fig. 7. Position (x_{33}), velocity ($\dot{x}_{33}$) and acceleration ($\ddot{x}_{33}$) of the floater in heave, for a ballast mass $m_b = 50000\,\mathrm{kg}$, under irregular wave conditions.

A plot of the floater's behaviour under these conditions is depicted in Fig. 7.

The calculation of the mean power production of the system follows the same procedure as before but now regarding the 20 min time window. For both ballast masses, the mean power production is, thus,

$$P_\mathrm{b}(m_\mathrm{b} = 50000\mathrm{kg}) = 14.7\ \mathrm{kW}$$

$$P_\mathrm{b}(m_\mathrm{b} = 70000\mathrm{kg}) = 16.1\ \mathrm{kW}$$

In this particular case, the wave energy converter exhibits a moderately better performance with the larger ballast mass compared to the lower mass. But it is essential to highlight that this outcome is subject to variability upon the specific location and prevailing wave climate, as evidenced by the results obtained. Therefore, site-specific characteristics play a pivotal role in determining the optimal ballast mass for achieving the optimal energy conversion performance.

IV. Conclusion

This study presents a novel wave energy converter system developed at IST, composed mainly of a floater and a ballast, connected by cables. A preliminary performance analysis is conducted, employing numerical simulations based on linear wave theory and regular and irregular wave conditions. By leveraging the system's axisymmetric nature, the analysis considers only the surge, heave, and pitch modes. Moreover, the hydrodynamic coefficients were obtained using WAMIT.

The results reveal significant nonlinear behavior during the floater's ascending phase when the ballast is moving in the energy accumulation step. Moreover, the findings demonstrate the converter's performance sensitivity to the ballast's mass, resulting in substantial variations in both the power production output and the operational range of wave periods.

In the context of wave energy conversion, the numerical modeling done in this work is based on linear water wave theory which has inherent limitations. One major drawback is its inability to incorporate energy losses caused by real fluid effects such as viscosity, turbulence and other dissipative effects.

To enhance future modeling efforts, further attention can be directed towards improving the cable model. Specifically, since the ballast is always vertically suspended at the cable's end, its vertical acceleration is a function of the vertical acceleration of the centre of mass of its rotational motion; thus, the transmitted force might not be vertical when the floater moves in the surge. Consequently, the transmitted force may not be entirely vertical when the floater moves in the surge. Finally, optimization of the floater's geometry stands as a potential avenue to improve energy extraction performance.

Acknowledgement

This research was partially supported by the Portuguese Foundation for Science and Technology - FCT, through IDMEC, under LAETA, project UIDB/50022/2020. The first author was supported by FCT grant no. DFA/BD/07315/2021.

References

[1] A. F. O. Falcão, "Phase control through load control of oscillating-body wave energy converters with hydraulic PTO system," *Ocean Engineering*, vol. 35, pp. 358–366, 03 2008.

[2] A. F. de O. Falcão, "Wave energy utilization: A review of the technologies," *Renewable and Sustainable Energy Reviews*, vol. 14, no. 3, pp. 899–918, 2010.

[3] A. Clément, A. Babarit, J.-c. Gilloteaux, C. Josset, and G. Duclos, "The SEAREV wave energy converter," in *Proceedings of the 6th Wave and Tidal Energy Conference, Glasgow, UK*, 01 2005.

[4] R. Yemm, D. Pizer, C. Retzler, and R. Henderson, "Pelamis: experience from concept to connection," *Philosophical Transactions of the Royal Society A: Mathematical, Physical and Engineering Sciences*, vol. 370, no. 1959, pp. 365–380, 2012.

[5] J. C. C. Henriques and J. M. C. S. André, "Power plant for wave energy conversion," Portuguese Patent PT104 885, Priority date 2011/12/15.

[6] W. E. Cummins, "The impulse response function and ship motions," *Schiffstechnik 9*, pp. 101–109, 1962.

[7] G. Duclos, A. H. Clément, and G. Chatry, "Absorption of Outgoing Waves In a Numerical Wave Tank Using a Self-Adaptive Boundary Condition," *International Journal of Offshore and Polar Engineering*, vol. 11, no. 03, 09 2001.

[8] J. C. C. Henriques, J. C. C. Portillo, W. Sheng, L. M. C. Gato, and A. F. O. Falcão, "Dynamics and control of air turbines in oscillating-water-column wave energy converters: Analyses and case study," *Renewable and Sustainable Energy Reviews*, vol. 112, pp. 571–589, 2019. [Online]. Available: https://www.sciencedirect.com/science/article/pii/S1364032119303168

[9] J. C. C. Henriques, M. F. P. Lopes, R. P. F. Gomes, L. M. C. Gato, and A. F. O. Falcão, "On the annual wave energy absorption by two-body heaving WECs with latching control," *Renewable Energy*, vol. 45, pp. 31–40, 2012. [Online]. Available: https://www.sciencedirect.com/science/article/pii/S0960148112001322

[10] Y. Goda, *Random Seas and Design of Maritime Structures*, 3rd ed. World Scientific, 2010.

[11] Newman, J. N. and Lee, C. H., "*WAMIT* user manual." [Online]. Available: https://www.wamit.com/manual.htm

[12] G. Paredes, F. Taveira-Pinto, M. Lopes, R. Gomes, and L. Gato, "Estudo experimental do corpo flutuante de um modelo de um sistema offshore de energia das ondas," in *3as Jornadas de Hidráulica, Recursos Hídricos e Ambiente*. Faculdade de Engenharia da Universidade do Porto, 2008.